



Seismic energy dissipation in bridges with air springs

A. Sherafati^a, F. Ahmadi^b and S. Maleki^{c,*}

a. *Department of Civil Engineering, University of Nebraska-Lincoln, Lincoln, Nebraska, USA.*

b. *Department of Civil Engineering, University of Texas at Austin, Austin, Texas, USA.*

c. *Room 431, Department of Civil Engineering, Sharif University of Technology, Tehran, P.O. Box 11155-9313, Iran.*

Received 17 May 2011; received in revised form 5 January 2015; accepted 7 March 2015

KEYWORDS

Bridges;
Seismic effects;
Energy dissipation;
Dampers;
Air springs.

Abstract. Seismic loads on bridges may cause large damaging forces in substructure. Isolation and energy dissipating elements or a combination of the two have been used to reduce the transmitted forces caused by seismic loading. The benefits of these systems are mainly attributed to the increase of structure's natural period of vibration and damping. This paper investigates a new device that works on the same principles. This device is composed of sliding bearings and air springs or airbags. Several bridges are analyzed using the Nishimura's model for air springs; and the sensitivity of seismic response of bridges due to variable spring parameters is investigated and optimum values are obtained. Then, using these parameters for the air spring and solving the equation of motion, the variation of air spring internal parameters with time are investigated. Results show that air springs are very efficient in reducing the effects of seismic forces.

© 2015 Sharif University of Technology. All rights reserved.

1. Introduction

Bridges are lifeline structures. Failure of bridges in a seismic event will seriously hamper the relief and rehabilitation work. There are many cases of damage to bridges in the past earthquakes all over the world. Due to their structural simplicity and non-redundancy, many bridges are particularly vulnerable to damage and even collapse when subjected to earthquakes. For very rigid structures, like single span bridges or continuous bridges with short piers, the period of free vibration is often very short. For such structures the earthquake response is at its peak value. The seismic forces on bridges can be reduced if the fundamental period of the bridge is lengthened and the energy dissipating capability is increased. Seismic isolation is an old design idea to counter the damaging effects of earthquakes. This innovative design approach aims mainly at the isolation of a structure from the supporting

ground, generally in the horizontal direction, in order to reduce the transmission of earthquake motion to the structure. One of the goals of the seismic isolation is to shift the fundamental frequency of a structure away from the dominant frequencies of earthquake ground motion. Often, an isolation system is enhanced with an energy dissipating device to reduce the demand on the structure. A variety of isolation devices including elastomeric bearings (with and without a lead core) and frictional slide bearings have been developed for bridges [1]. Ghobarah and Ali [2] studied elastomeric bearings in seismic isolation of bridges and showed that these devices are quite effective in reducing the seismic response. In another study, Jangid [3] investigated the stochastic response of bridges seismically isolated with lead-rubber bearings. Experimental studies on bridges isolated by sliding bearings with displacement control devices to real earthquake ground motion were carried out by Constantinou et al. [4] and Tsopelas et al. [5]. The effectiveness of friction pendulum system has also been studied by several researchers [6-8]. Air springs have been used as a damper and shock resisting element in the industry for decades [9-13]. In this paper, the

*. *Corresponding author. Tel.: +98 21 66164251;
Fax: +98 21 66014828
E-mail address: smaleki@sharif.edu (S. Maleki)*

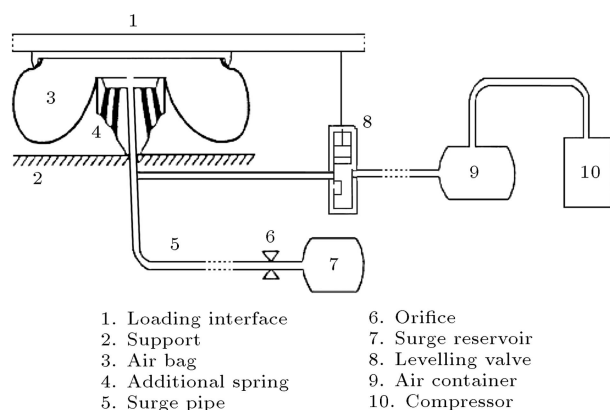


Figure 1. Typical pneumatic spring system [14].

application of air springs to bridges is investigated analytically. It is shown that, if installed correctly, these devices are capable of lengthening the natural period of bridges and increase damping. Components in the substructure can benefit the most from these merits.

2. Using air as a damper

A pneumatic spring is a spring which employs gas as its resilient element (Figure 1) [14]. Since the gas is usually air, such a spring is often called an air spring. The ability of the air spring to support a given mass is governed by the effective area and the confined gas pressure. The compressibility of the gas provides the desired elasticity for the spring. One of the advantages of the air spring is that the energy-storage of air is far greater per unit weight than that of a mechanical spring material, such as steel and rubber. Because of the efficient potential energy storage of air springs, their use in a vibration-isolation system can result in a natural frequency for the system which is about 10 times lower than that for a system employing vibration isolators made from steel and rubber. The axial stiffness of an air spring is inversely proportional to the volume. The air spring softens in the vertical direction with increasing volume. To increase the volume and lower the stiffness of an air spring, an air reservoir may be connected to it via a passageway. The increased volume reduces the natural frequency as the square root of increased volume. In the simplest case, the air spring system consists of an air bellow that is connected to an auxiliary volume via a pipe (Figure 1).

When the system is exposed to vibration, the air inside the bellow is compressed (or expanded) and the pressure difference between the bellow and the auxiliary volume rises. Interchange of air through the surge pipe can neutralize the pressure difference.

All gases heat up when compressed and cool down when expanded. If the air spring is stroked so slowly that all of the heat generated during compression (or

absorbed during expansion) is dissipated, the process is called an isothermal (constant temperature) process. If a pneumatic spring is stroked fast enough that all of the heat of the operation is conserved it would be an adiabatic process. Actually, a rapid spring deflection results in an adiabatic compression with a higher pressure and a higher spring rate, whereas a slow deflection results in an isothermal compression having the opposite effect. Effective area (A_e) is the load-carrying area of a pneumatic spring at a given point in the stroke. Phrased another way, it is the load on the spring divided by the air pressure in the spring. For a piston in a cylinder, the effective area of the spring is constant, but the effective area of a flexible air spring (or air bag) may change during its stroke. To determine the load at each moment, the gauge pressure (P_g) should be used in calculations. It means that the pressure of free air (P_o) must be subtracted from the absolute pressure (P_a) inside the system. The conventional absolute internal pressure of industrial air springs varies between 400 to 800 kPa. Therefore, the gauge pressure would be between 300 to 700 kPa. Finally, the force exerted from the spring to the mass it supports would be the product of gauge pressure and effective area.

Generally, there are two kinds of damping associated with air springs due to the flow of air between the bag and the reservoir. These are capillary and orifice damping. Capillary damping is due to the resistance of the surge pipe against flow, and orifice damping appears when the flow passes through the orifice [9].

Airbags are similar to air springs in concept, and are commonly used in automobile safety restraint system. Allen Breed was holding the patent to the only crash sensing technology available at the birth of the airbag industry [15]. Breed invented a “sensor and safety system” in 1968; the world’s first electromechanical automotive airbag system. When a sensor in the car detects a strong collision, it sends an electric current to a wire. The wire heats up, and the charge in the inflator undergoes a chemical reaction, producing a gas that rapidly inflates the bag. Several new applications for airbags are being investigated due to their low frequency and shock absorbing characteristic. For instance, airbags are employed as shock absorbers in an earth-landing device [16].

3. Nishimura’s structural model for air springs

Several analytical models for air springs have been suggested and employed by commercial software [10–13]. A well-known analytical model for air springs is the Nishimura’s model, which is employed by ADAMS [17] in simulation of air springs. The Nishimura air spring is not a one-volume assumption and can therefore be used to model orifice damping and flow resistance through

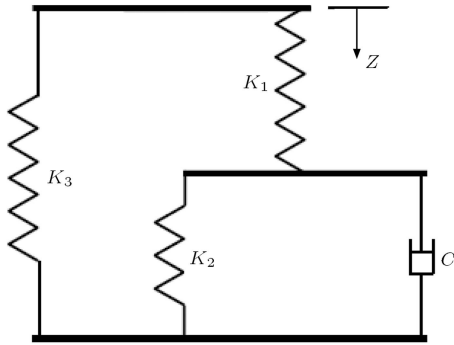


Figure 2. Nishimura's model for an air spring.

the pipe. The Nishimura's model, for a system, as shown in Figure 2, consists of three springs and a damper. The springs' stiffnesses and the damping constant are defined as follows:

$$K_1 = \gamma \cdot (A_e)^2 \cdot \frac{p_o}{V_r}, \quad (1)$$

$$K_2 = \gamma \cdot (A_e)^2 \cdot \frac{p_o}{V_b}, \quad (2)$$

$$K_3 = p_{go} \cdot \frac{dA_e}{dz} = (p_o - p_a) \cdot \frac{dA_e}{dz}, \quad (3)$$

$$C = R_f \cdot A_e^2 \cdot \rho_o \cdot g = \frac{0.126}{d_s^3} \cdot A_e^2 \cdot \rho_o \cdot g, \quad (4)$$

where d_s is the diameter of the surge pipe in meters (m); g is the acceleration due to gravity (m/s^2); R_f is the flow resistance coefficient; A_e is the effective area (m^2); V_b is the airbag volume (m^3); V_r is the reservoir volume (m^3); ρ_o is the mean density of the air (kg/m^3); p_o is the initial absolute pressure (Pa); p_{go} is the initial gauge pressure (Pa); p_a is the atmospheric pressure (Pa); and γ is a factor related to the loading frequency and therefore, related to the thermodynamic process in the system. When the system undergoes a very rapid loading, adiabatic process occurs, and γ is assumed to be equal to 1.4. On the other hand, in slow loading which leads to isothermal process, γ approaches 1. The stiffness is related to the change in the effective area. In this paper, it is assumed that the effective area of the air spring remains constant, i.e. $K_3 = 0$. Due to its simplicity and accuracy, Nishimura's model has been used extensively in the analysis of air supported systems.

4. Application of air springs to bridges

Consider a single-span slab-girder bridge as shown in Figure 3. Figure 3(a) shows a possible location for mounting the air springs to mitigate transverse vibration. Similarly, Figure 3(b) shows a possible device mounting for longitudinal vibration. It is assumed that the girders rest on slide bearings with negligible

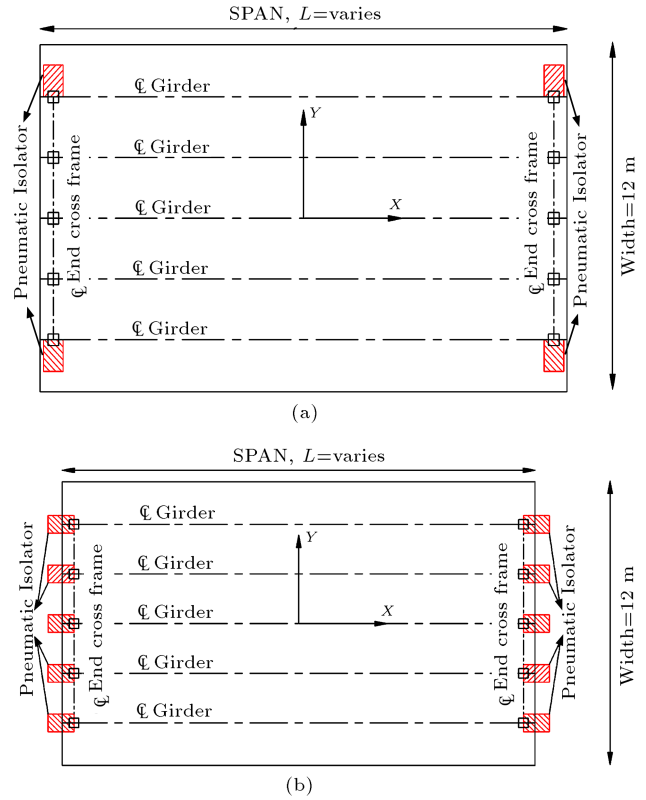


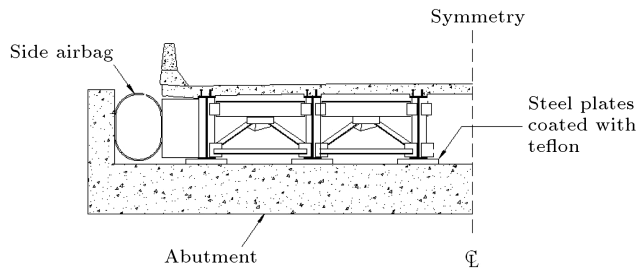
Figure 3. (a) Lateral, and (b) longitudinal isolators installment.

friction and do not restrain the horizontal motion of the bridge. Therefore, in an earthquake, the bridge inertia loads push the bridge against the devices in two perpendicular directions. The device reaction is transmitted to the substructure. If designed properly, this reaction should be much lower than that for a bridge without the device, as this system effectively increases the natural frequency of the system. However, the bridge superstructure's displacement increases and should remain tolerable. In addition, design of the bag and the orifice should consider sudden increases in the internal pressure of the bag due to seismic loading. Note that to engage the device, sliding bearings are required in parallel to the air springs.

To investigate the effectiveness of air devices, several analytical models of slab-girder bridges are made. The properties of these bridges are described in Table 1. The span of these bridges covers the practical range of slab-girder bridges. Due to symmetry and also high in-plane rigidity of the deck, the total mass of the deck can be lumped at its center of mass [18]. As shown in Figure 4, the air spring is mounted such that it acts in series with the end diaphragms of the bridge. The bridges are modeled using the Nishimura's model of air spring for the transverse vibration. Figure 5 illustrates the proposed structural model. In this model, M is the total mass of the superstructure and, K_c is the stiffness of the end diaphragm.

Table 1. Bridge properties used in analyses.

Bridge model number	Span (m)	Width (m)	Deck thickness (m)	Girder size (U.S. standard)	Total elastomer K_e (kN/mm)	Total cross-frame K_c (kN/mm)	Weight (kN)
1	13	12	0.19	W30×99	10	1620	865
2	18	12	0.19	W40×221	10	1620	1300
3	21	12	0.19	W40×268	10	1620	1800
4	30	12	0.19	W40×268	10	1620	2600

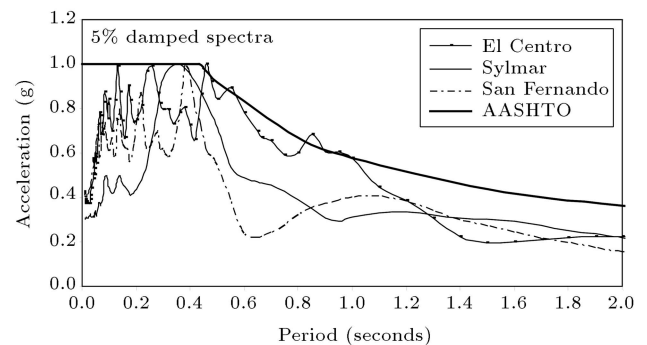
**Figure 4.** Lateral view of isolated bridge above the abutment.

The models are subjected to the 1940 El Centro ground motion. This ground motion with peak ground acceleration of 0.34 g is widely accepted as a typical design level earthquake and is used as such in this study. Except for very short periods, this ground motion, with 5% damping, agrees well with the American Association of State Highway and Transportation Officials [19] design response spectrum for seismic zone 4 ($A = 0.4$) and soil type II ($S = 1.2$). To consider other earthquakes with different frequency contents and intensity, the 1994 Northridge (Sylmar County) time-history with peak ground acceleration of 0.84 g, and the 1971 San Fernando (Pacoima Dam) time-history with peak ground acceleration of 1.25 g are also used in subsequent analyses (Table 2). The scaled spectra are such that the peak response of all earthquakes matches the peak of AASHTO's response spectrum. Figure 6 shows the plot of acceleration response spectra of scaled earthquakes.

The response of the bridge with fixed lateral support is presented in Figure 7. By comparing the

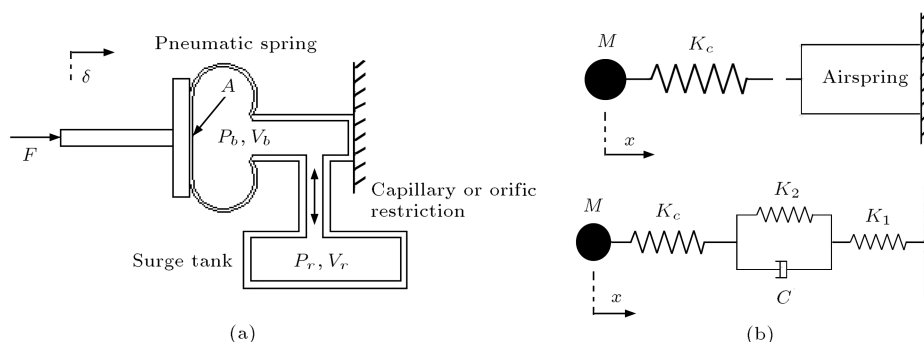
Table 2. Ground motions used in time-history analyses.

Scale factor	PGA	Record
1.18	0.34 g	El Centro 1998
0.36	0.84 g	Northridge (Sylmar County) 1994
0.33	1.25 g	San Fernando (Pacoima Dam) 1971

**Figure 6.** Scaled response spectra for type II soil and ground acceleration of 0.4g and 5% damping ratio.

base shear force presented in Figure 7(b) with the bridges equipped with the proposed isolation device, one can conclude that this system can effectively reduce the transmitted forces to the substructure. For instance, the minimum shear force for the fixed lateral support in the case of El-Centro earthquakes is about 500 kN, which is reduced to less than 35 kN by using the isolation device (see Figures 8 and 11).

In the air spring model, the seismic loading frequency is slow, and γ can be assumed to be 1.

**Figure 5.** (a) An air spring, and (b) Nishimura structural model of an isolated bridge.

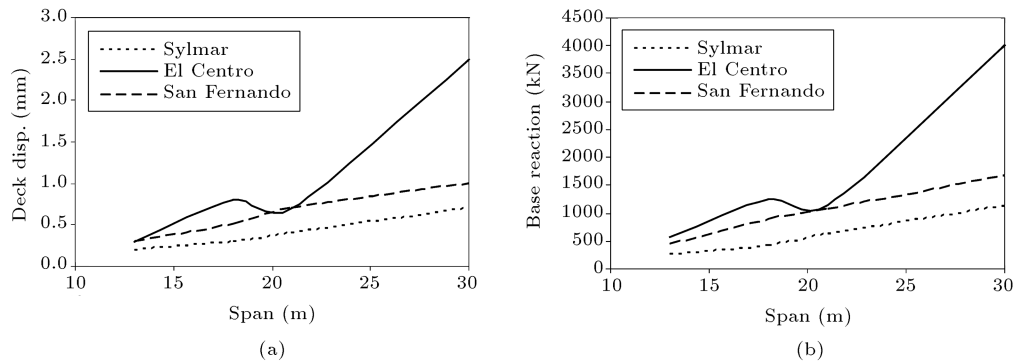


Figure 7. (a) Deck displacement, and (b) reaction force for non-isolated bridge.

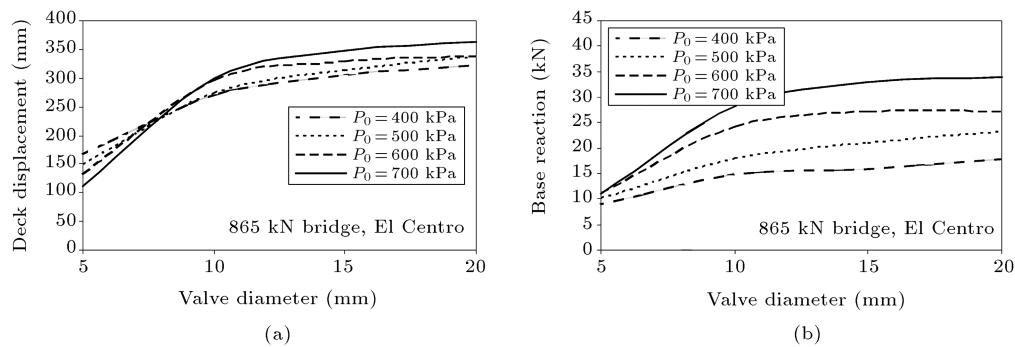


Figure 8. Structural response for El Centro earthquake under changing orifice diameter: (a) Deck displacement; and (b) reaction force.

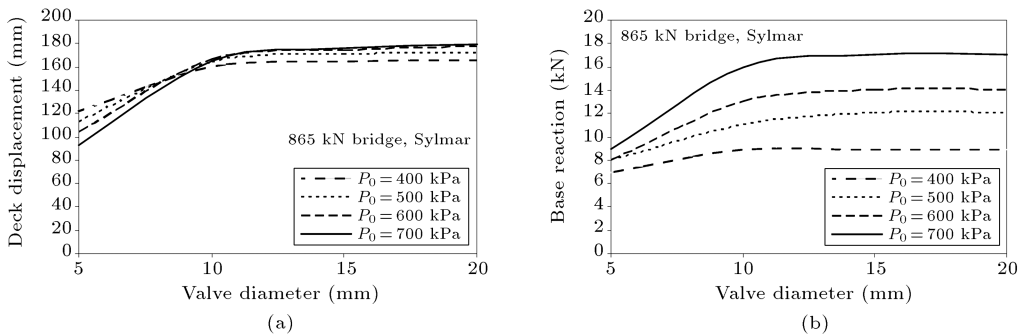


Figure 9. Structural response for Sylmar earthquake under changing orifice diameter: (a) Deck displacement; and (b) reaction force.

Also, the change in area is ignored, i.e. $K_3 = 0$. The initial volumes of the bag and the reservoir are assumed to be equal to 0.03 m^3 , which is a conventional value for this parameter. Stiffnesses K_1 and K_2 , and damping C are determined from Eqs. (1), (2) and (4), respectively. A series of linear dynamic time history analyses are performed on the model bridges with SAP program [20]. Analyses consider three variable parameters: orifice diameter (d_s), initial internal pressure (P_0), and effective area (A_e). Results for reaction to the substructure and superstructure's displacement are shown in Figures 8 through 13. Other bridges behave similarly and are not shown for the sake of brevity.

Results of analyses for an effective area of 0.09 m^2 are shown in Figures 8 through 10 for the 13 m

(865 kN weight) bridge. It is observed that with a decrease in d_s , deck displacement decreases. This is due to the increase in stiffness of the isolated system. Moreover, our investigations show that when using small orifice diameter, larger internal pressure results in smaller displacements. On the other hand, in the cases considered, the reaction forces do not vary substantially for diameters over 100 mm.

Figures 11 through 13 illustrate the results of analyses for all bridges for $P_0 = 700 \text{ kPa}$ and $d_s = 5 \text{ mm}$. It is seen that an increase in A_e causes smaller displacements and larger reaction forces. After a large number of analyses, $d_s = 5 \text{ mm}$, $P_0 = 700 \text{ kPa}$ and $A_e = 0.09 \text{ m}^2$ are chosen as optimum values of these parameters for considered bridges. In other words,

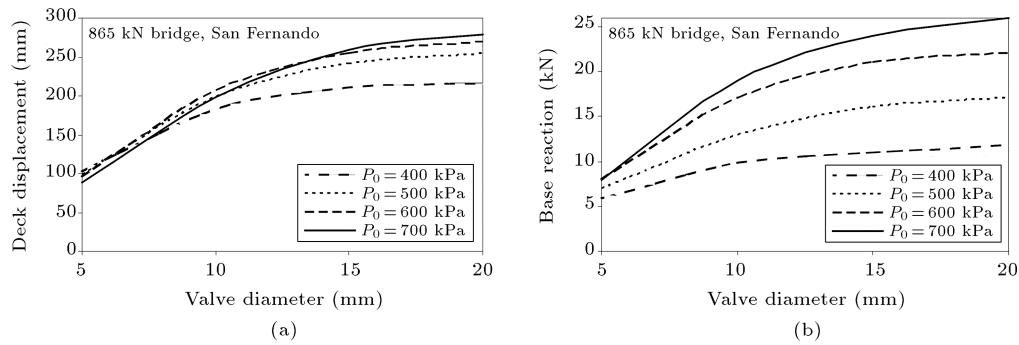


Figure 10. Structural response for San Fernando earthquake under changing orifice diameter: (a) Deck displacement; and (b) reaction force.

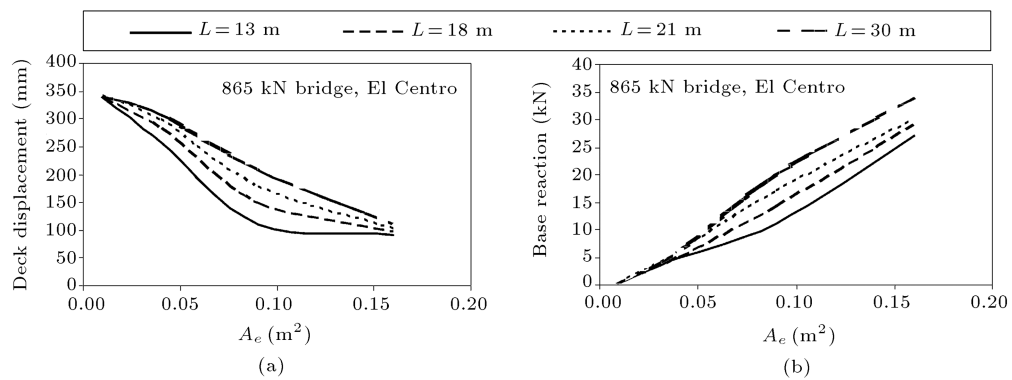


Figure 11. Structural response for El Centro earthquake ($d_s = 5$ mm and $P = 700$ kPa) vs. bag effective area: (a) Deck displacement; and (b) reaction force.

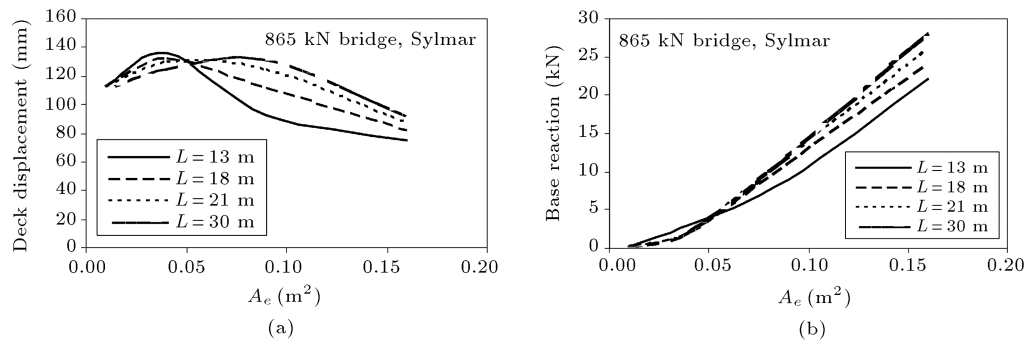


Figure 12. Structural response for Sylmar earthquake ($d_s = 5$ mm and $P = 700$ kPa) vs. bag effective area: (a) Deck displacement and (b) reaction force.

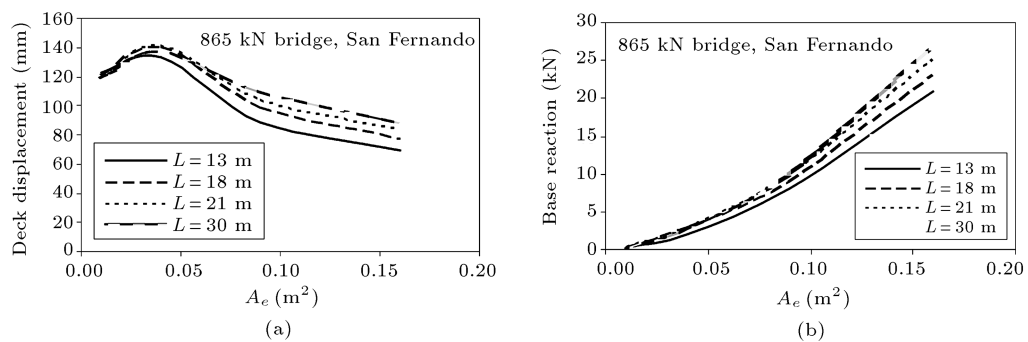


Figure 13. Structural response for San Fernando earthquake ($d_s = 5$ mm and $P = 700$ kPa) vs. bag effective area: (a) Deck displacement; and (b) reaction force.

these values for the air spring cause the most reduction in reaction force without excessive deck displacement. The Nishimura's model used in this investigation is simple and gives responses and reaction forces. It also proves that air springs are very effective in reducing the seismic demand. However, internal air spring parameters, such as pressure change with time, cannot be investigated with this model. This will be done in the next section by solving the equation of motion, numerically.

5. Time history analysis of structures with air springs

In order to investigate the air flow from the bag to the reservoir and vice versa in an air spring, a simple one Degree Of Freedom (DOF) mass-spring-damper model for the air spring shown in Figure 5 is developed and solved using the SIMULINK (a graphical interface of MATLAB) [21]. This software is capable of solving ordinary differential equations with initial conditions, numerically. The development of spring and damper properties for the model is described herein.

Knowing that in slab-girder bridges, the stiffnesses of end diaphragms are much larger than that of the air spring, and that they act in series, the stiffnesses of the end diaphragms are ignored and only that of air spring is considered [22]. The equation of motion can be written as:

$$M\ddot{x} + 2M\omega\xi\dot{x} + Kx = -M\ddot{x}_g, \quad (5)$$

where the spring force (F_z) in this equation is:

$$F_z = Kx = \left(\frac{pA_e^2\gamma}{V_b + V_r} + p_g \frac{dA_e}{dx} \right) x. \quad (6)$$

In Eq. (5), the spring force term can be evaluated at each instant of time corresponding to instantaneous bag pressure. In the simplified air spring system, the force balance for the piston can be expressed as:

$$F_z = A_e p_b - A_e p_a. \quad (7)$$

Substituting the above equation in Eq. (5), the general equation of motion can be rewritten as:

$$M\ddot{x} + 2M\omega\xi\dot{x} + (P_b - P_a)A_e = -M\ddot{x}_g. \quad (8)$$

Now the nonlinear parameters K and C can be obtained by means of thermodynamics and fluid mechanics principles. As mentioned before, the thermodynamic process in the loading of an air spring is assumed to be adiabatic, hence:

$$PV^\gamma = mRT_o. \quad (9)$$

Differentiating the equation above with respect to time gives the energy equation:

$$P_b \frac{dV_b}{dt} + \frac{V_b}{\gamma} \frac{dP_b}{dt} = \dot{m}RT_o. \quad (10)$$

The rate of mass flow \dot{m} between the bag and the reservoir from the orifice is [23]:

$$\dot{m} = A_t \sqrt{\left(\frac{2\gamma}{\gamma-1} \right) P_b \rho_1 \left(\frac{P_r}{P_b} \right)^{2/\gamma} \left[1 - \left(\frac{P_r}{P_b} \right)^{(\gamma-1)/\gamma} \right]},_{P_r < P_b} \quad (11)$$

where, A_t is the area of throat or orifice (m^2); P is pressure (Pa); ρ is density (kg/m^3); γ is specific heat ratio (for air $\gamma = 1.4$); and subscripts b and r indicate bag and reservoir, respectively. The maximum value of mass flow is:

$$\dot{m}_{\max} = \frac{A_t P_b}{\sqrt{T_0}} \sqrt{\frac{\gamma}{R} \left(\frac{2}{\gamma+1} \right)^{\frac{\gamma+1}{\gamma-1}}}, \quad (12)$$

where, T_0 is absolute temperature of the bag's air (K), and R is gas constant ($\text{J}/\text{kg}\cdot\text{K}$).

At every moment, the total mass of the air inside the bag and the reservoir is constant and equal to the initial value. The volume of the reservoir is also constant. Hence:

$$m_o = m_b + m_r = \frac{P_0(V_{bo} + V_r)^\gamma}{RT_0} = \text{const}, \quad (13)$$

$$P_r = \frac{m_r RT_0}{V_r^\gamma}. \quad (14)$$

The derived equations above can be solved numerically in SIMULINK and instantaneous values of the internal system parameters can be obtained.

In all SIMULINK models, it is assumed that $P_o = 700$ kPa and initial volumes are $V_{bo} = V_{ro} = 0.03$ m^3 . These were obtained as optimum values for considered bridges in the previous section. Catalogues of industrial air springs show that the volume of the bag is usually a linear function of its height, i.e.:

$$V_b = f(x) = V_{bo}(1 - ax), \quad a < 1. \quad (15)$$

For our example, the equation of the volume of the bag is assumed as:

$$V_b = 0.1 \times (0.3 - x). \quad (16)$$

Figures 14 through 19 illustrate the results of SIMULINK analyses for the 1300 kN bridge subjected to El Centro ground motion. The orifice diameter is 5 mm and the effective area of the bag is 0.09 m^2 . The advantage of this model is its ability to consider

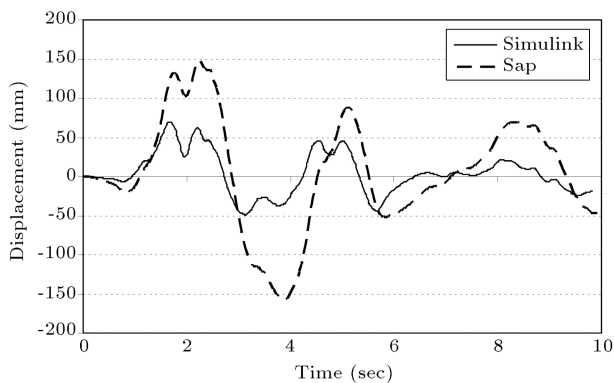


Figure 14. Deck displacement time history under El Centro ($W = 1300$ kN and $d_s = 5$ mm).

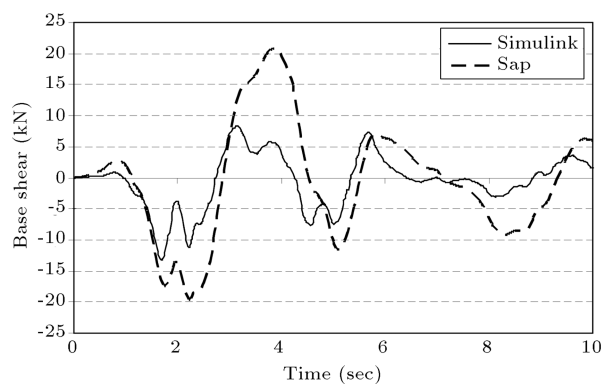


Figure 15. Base shear time history under El Centro ($W = 1300$ kN and $d_s = 5$ mm).

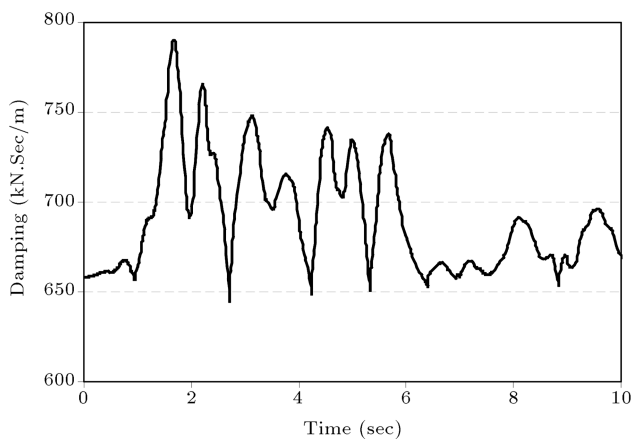


Figure 16. Damping time history under El Centro ($W = 1300$ kN and $d_s = 5$ mm).

the thermodynamic characteristics of the system with instantaneous stiffness and damping. It can also produce the time history response of internal system parameters such as air bag volume and pressure change. As seen in Figures 14 and 15, the deck displacement and base shear have reduced substantially when compared to SAP2000 results with the Nishimura's model. Note that in the Nishimura's model the stiffnesses of the springs and damper value are constant and based

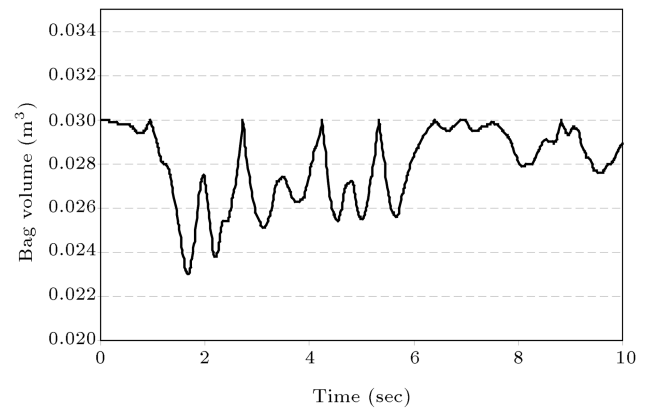


Figure 17. Bag volume time history under El Centro ($W = 1300$ kN and $d_s = 5$ mm).

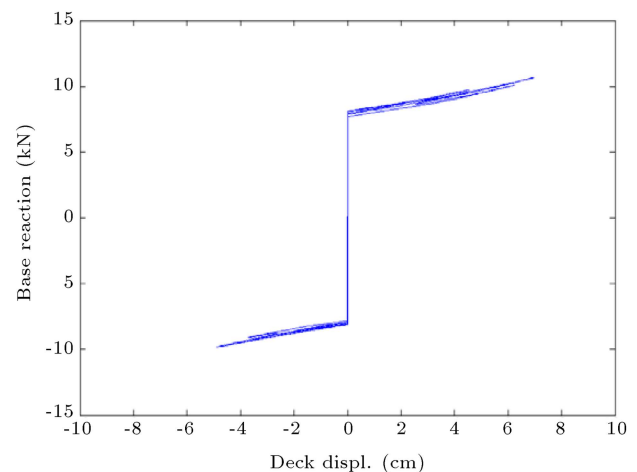


Figure 18. Force vs. displacement under El Centro ($W = 1300$ kN and $d_s = 5$ mm).

on initial values, whereas in the problem solved in SIMULINK, these parameters are updated based on instantaneous values of pressure and air travel through the orifice.

In Figure 16, the instantaneous damping is plotted against time. The initial damping value is assumed to be equivalent to the Nishimura's model (Eq. (4)). In Figure 17, the time history of the bag volume is plotted. The damping increases with decreasing bag volume.

The force-displacement relationship of the deck mass is shown in Figure 18. The figure indicates that the stiffness of an isolated bridge is nonlinear.

In Figure 19, the time variation of the bag and reservoir pressures is compared for orifice diameters of 5 mm and 30 mm. It is seen that by increasing the orifice diameter, the resistance against air flow between the bag and the reservoir decreases and, as a result, the damping decreases. It appears that there is no air resistance in the case of $d_s = 30$ mm in which the reservoir and the bag volumes act as one [24,25]. By decreasing d_s , the flow of air is restricted and a difference between the internal pressures of the two

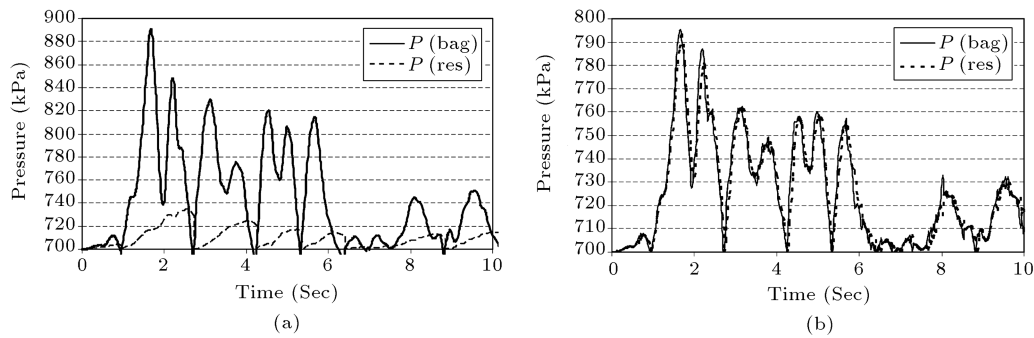


Figure 19. Bag and reservoir pressure time history under El Centro ($W = 1300$ kN): (a) $d_s = 5$ mm; and (b) $d_s = 30$ mm.

volumes is observed. For very small values of d_s , the reservoir practically does not affect the internal pressure of the bag. This indicates that the Nishimura's model may fail to be accurate in such cases. In addition, the instantaneous internal pressure of the bag may exceed the permissible value, and the fabric of the bag may explode. Therefore, very small values of d_s are not practical for use in an airbag device.

6. Conclusions

Based on the analytical study presented in this paper, the following conclusions can be drawn.

Air springs can highly increase the natural period of a structure due to their low stiffness. In particular, for bridges considered in this study, the period rises up to 7 seconds. On the other hand, by decreasing the orifice diameter (d_s), which is the main parameter in energy dissipation, the damping increases.

If $d_s > 30$ mm, the internal pressure of the bag and the reservoir will be approximately the same. This means that there is no resistance against air flow and both volumes act as one. In this case there is no beneficial damping.

By using air spring dampers in typical bridges, reaction forces decrease substantially. This is due to decrease in stiffness and increase in damping and natural period of the system. Results show that this system highly reduces the exerted forces on to the substructure.

Analyses show that by decreasing d_s , the input energy increases and the main part of it is dissipated by damping. However, as d_s increases, hysteresis loops appear to grow, and a part of input energy is dissipated as spring energy.

The air damper considered in this paper can be thought of as a passive anti-seismic device. Considering that the main parameter in damping is the orifice diameter, by changing d_s during seismic loading a semi-active device can be developed and results can be further improved. This can be considered as a part of future research. Also, experimental verification of

the device and comparison of system performance with other devices are necessary.

References

1. Kunde, M.C. and Jangid, R.S. "Seismic behavior of isolated bridges: A-state-of-the-art review", *Electronic Journal of Structural Engineering*, **3**, pp. 140-170 (2003).
2. Ghobarah, A. and Ali, H.M. "Seismic performance of highway bridges", *Engineering Structures*, **10**(3), pp. 157-166 (1988).
3. Jangid, R.S. "Equivalent linear stochastic seismic response of isolated bridges", *Journal of Sound and Vibration*, **309**(3-5), pp. 805-822 (2008).
4. Constantinou, M.C., Kartoum, A., Reinhorn, A.M. and Bradford, P. "Sliding isolation system for bridges. Experimental study", *Earthquake Spectra*, **8**(3), pp. 321-321 (1992).
5. Tsopelas, P., Constantinou, M.C., Okamoto, S., Fujii, S. and Ozaki, D. "Experimental study of bridge seismic sliding isolation systems", *Engineering Structures*, **18**(4), pp. 301-310 (1996).
6. Kartoum, A., Constantinou, M.C. and Reinhorn, A.M. "Sliding isolation system for bridges. Analytical study", *Earthquake Spectra*, **8**(3), pp. 345-345 (1992).
7. Wang, Y.-P., Chung, L.-L. and Liao, W.-H. "Seismic response analysis of bridges isolated with friction pendulum bearings", *Earthquake Engineering and Structural Dynamics*, **27**(10), pp. 1069-1093 (1998).
8. Jangid, R.S. "Stochastic response of bridges seismically isolated by friction pendulum system", *Journal of Bridge Engineering*, **13**(4), pp. 319-330 (2008).
9. Henderson, R.J. and Raine, J.K. "A two-degree-of-freedom ambulance stretcher suspension. Part 2: Simulation of system performance with capillary and orifice pneumatic damping", *Proceedings of the Institution of Mechanical Engineers, Part D: Journal of Automobile Engineering*, **212**, pp. 227-240 (1998).
10. Berg, M. "Modeling of springs and dampers for dynamic analysis of rail vehicles - a pilot study", Report ISRN KTH/FKT/FR-94/51-SE, KTH, Stockholm (1994).

11. Berg, M. "An air spring model for dynamic analysis of rail vehicles", Report TRITA-FKT Report 1999:32, Royal Institute of Technology, Stockholm (1999).
12. Berg, M. "Three-dimensional air spring model with friction and orifice damping", *Proceedings of 16th LAVSD Symposium, The Dynamics of Vehicles on Roads and on Tracks*, Pretoria, pp. 528-539 (2000).
13. Eaton, M. "A mathematical model of a nonlinear pneumatic suspension system", Report BD/TR/97/008, ABB Daimler-Benz Transportation (Rolling Stock) Ltd (1997).
14. Hirtreiter, A.B. "Principles and application of pneumatic springs", *SAE Special Publications*, pp. 33-37 (1973).
15. Krueger, S. and Gessner, W., *Advanced Microsystems for Automotive Applications*, Yearbook 2002: Springer (2002).
16. Gardinier, D.J. and Taylor, A.P. "Design and testing of the K-1 reusable launch vehicle landing system airbags", *Proceedings of AIAA 15th Aerodynamic Decelerator Conference*, Toulouse, France (1999).
17. *Automated Dynamic Analysis of Mechanical Systems (ADAMS)*, MSC Software Corporation, New Port Beach, CA, USA (2010).
18. Maleki, S. "Effect of diaphragms on seismic response of skewed bridges", *Proceedings of the First MIT Conference on Computational Fluid & Solid Mechanics*, Cambridge, MA, pp. 681-684 (2001).
19. AASHTO-LRFD. American Association of State Highway and Transportation Officials, Washington, D.C. (2010).
20. Sap2000 version 8.03, Computers and Structures Inc., Berkeley, CA.
21. SIMULINK toolbox for MATLAB MathWorks Inc. (1996).
22. Maleki, S. "Deck modeling for seismic analysis of skewed slab-girder bridges", *Engineering Structures*, **24**, pp. 1315-1326 (2002).
23. Wang, X. and Zhang, Y. "Development of a critical air flow venturi for air sampling", *Journal of Agricultural Engineering AP*, **73**(3), pp. 257-264 (1999).
24. *LS DYNA Theoretical Manual*, Livermore Software Technology Corporation, Livermore, CA (1998).
25. Deprez, K., Moshou, D., Hostens, I., Anthonis, J. and Ramon, H. "Hardware design and optimization of a 1 DOF suspension", *Proceedings of Fourth International Symposium on Mathematical Modeling and Simulation in Agricultural and Bio-Industries*, Haifa, Israel (2001).

Biographies

Ardalan Sherafati started his university studies in Sharif University of Technology (SUT), Tehran, Iran, in the field of Civil Engineering in September 1999. Having finished his undergraduate study in 2003, he continued his studies as a graduate student at SUT in Structural Engineering. He successfully defended his thesis titled "Air Spring Dampers" to obtain his MS degree in November 2006. He was accepted as a PhD student at the University of Nebraska-Lincoln, USA, in 2007, where he worked on jointless bridges. He has coauthored several papers in area of bridge engineering. He is currently a Project Engineer at BlueScope Construction Inc. in Kansas City, Missouri.

Farhad Ahmadi started his Master[s degree in Structural Engineering at Sharif University of Technology, in Tehran, Iran. He continued his education in the University of Texas at Austin, USA, where he obtained his PhD in Structural Engineering. He has been working in the industry in the US ever since.

Shervin Maleki obtained his BS and MS Degrees from the University of Texas at Arlington with honor. He then pursued his PhD degree at the New Mexico State University and finished it in 1988. He has many years of experience in structural design both in the US and Iran. He has been a faculty member at Bradley University in Illinois, USA, and Sharif University of Technology in Tehran, Iran. He has authored and coauthored over fifty technical papers and has authored two books and a chapter in the Handbook of International Bridge Engineering, in 2013. His research area is mainly focused on seismic design of bridges and buildings. He has also patented several seismic metallic yielding dampers.